JACC: CARDIOVASCULAR IMAGING VOL. ■, NO. ■, 2020
© 2020 BY THE AMERICAN COLLEGE OF CARDIOLOGY FOUNDATION
PUBLISHED BY ELSEVIER

ORIGINAL RESEARCH

Diagnostic Accuracy of [^{11}C]PIB Positron Emission Tomography for Detection of Cardiac Amyloidosis

Sara Rosengren, MD,[a,*] Tor Skibsted Clemmensen, MD, PhD,[b,*] Lars Tolbod, PhD,[c] Sven-Olof Granstam, MD, PhD,[d] Hans Eiskjær, MD, PhD,[b] Gerhard Wikström, MD, PhD,[e] Ola Vedin, MD, PhD,[e] Tanja Kero, MD, PhD,[f] Mark Lubberink, PhD,[f,g] Hendrik J. Harms, PhD,[c] Frank A. Flachskampf, MD, PhD,[d] Tomasz Baron, MD, PhD,[d] Kristina Carlson, MD, PhD,[a] Fabian Mikkelsen, MD,[b] Gunnar Antoni, PhD,[h] Niels Frost Andersen, MD, PhD,[i] Steen Hvitfeldt Poulsen, MD, PhD,[b] Jens Sörensen, MD, PhD[c,f]

ABSTRACT

OBJECTIVES This dual-site study evaluated the diagnostic accuracy of the method.

BACKGROUND Pittsburgh compound ([^{11}C]PIB) positron emission tomography (PIB-PET) has shown promise as a specific and noninvasive method for the diagnosis of cardiac amyloidosis (CA).

METHODS The study had 2 parts. In the initial study, 51 subjects were included, 36 patients with known CA and increased wall thickness (15 immunoglobulin light chain [AL] and 21 transthyretin [ATTR] amyloidosis) and 15 control patients (7 were non-amyloid hypertrophic and 8 healthy volunteers). Subjects underwent PIB-PET and echocardiography. Sensitivity and specificity of PIB-PET were established for 2 simple semiquantitative approaches, standardized uptake value ratio (SUVR) and retention index (RI). The second part of the study included 11 amyloidosis patients (5 AL and 6 hereditary ATTR) without increased wall thickness to which the optimal cutoff values of SUVR (>1.09) and RI (>0.037 min^{-1}) were applied prospectively.

RESULTS The diagnostic accuracy of visual inspection of [^{11}C]PIB uptake was 100% in discriminating CA patients with increased wall thickness from controls. Semiquantitative [^{11}C]PIB uptake discriminated CA from controls with a 94% (95% confidence interval [CI]: 80% to 99%) sensitivity for both SUVR and RI and specificity of 93% (95% CI: 66% to 100%) for SUVR and 100% (95% CI: 75% to 100%) for RI. [^{11}C]PIB uptake was significantly higher in AL-CA than in ATTR-CA patients ($p < 0.001$) and discriminated AL-CA from controls with 100% (95% CI: 88% to 100%) accuracy for both the semiquantitative measures. In the prospective group without increased wall thickness, RI was elevated compared to controls ($p = 0.001$) and 5 of 11 subjects were evaluated as [^{11}C]PIB PET positive.

CONCLUSIONS In a dual-center setting, [^{11}C]PIB PET was highly accurate in detecting cardiac involvement in the main amyloid subtypes, with 100% accuracy in AL amyloidosis. A proportion of amyloidosis patients without known cardiac involvement were [^{11}C]PIB PET positive, indicating that the method may detect early stages of CA. (J Am Coll Cardiol Img 2020;■:■–■) © 2020 by the American College of Cardiology Foundation.

From the [a]Department of Medical Sciences, Hematology, Uppsala University, Uppsala, Sweden; [b]Department of Cardiology, Aarhus University Hospital, Aarhus, Denmark; [c]Department of Nuclear Medicine and PET, Aarhus University Hospital, Aarhus, Denmark; [d]Department of Medical Sciences, Clinical Physiology, Uppsala University, Uppsala, Sweden; [e]Department of Medical Sciences, Cardiology, Uppsala University, Uppsala, Sweden; [f]Department of Surgical Sciences, Radiology, Uppsala University, Uppsala, Sweden; [g]Department of Medical Physics, Uppsala University, Uppsala, Sweden; [h]Department of Medicinal Chemistry, Uppsala University, Uppsala, Sweden; and the [i]Department of Hematology, Aarhus University Hospital, Aarhus, Denmark. *Drs. Rosengren and Skibsted Clemmensen contributed equally to this work. This study received funding from the Swedish Heart-Lung Foundation, Stockholm, Sweden (registration number 20160746). All authors have reported that they have no relationships relevant to the contents of this paper to disclose.

The authors attest they are in compliance with human studies committees and animal welfare regulations of the authors' institutions and Food and Drug Administration guidelines, including patient consent where appropriate. For more information, visit the *JACC:* Cardiovascular Imaging author instructions page.

Manuscript received June 13, 2019; revised manuscript received February 11, 2020, accepted February 11, 2020.

ISSN 1936-878X/$36.00 https://doi.org/10.1016/j.jcmg.2020.02.023

ABBREVIATIONS AND ACRONYMS

AL = immunoglobulin light chain amyloidosis

ATTR = transthyretin amyloidosis

AUC = area under the curve

CA = cardiac amyloidosis

CI = confidence interval

IQR = interquartile range

IVST = interventricular septum thickness

LVEF = left ventricular ejection fraction

MRI = magnetic resonance imaging

NYHA = New York Heart Association

PET = positron emission tomography

PIB = Pittsburgh compound B

RI = retention index

ROC = receiver operating curve

SUVR = standardized uptake value ratio

TAPSE = tricuspid annular plane systolic excursion

Amyloidosis is a group of diseases characterized by misfolded protein deposition in various organs, leading to progressive organ failure. The 2 most prevalent types are immunoglobulin light chain (AL) and transthyretin (ATTR) amyloidosis. In both these forms, the heart is commonly involved, causing increased myocardial wall thickness and eventually heart failure. Patients with advanced cardiac amyloidosis (CA) have poor outcome, especially in severe AL-CA, where survival is short despite treatment. Diagnosis is often delayed because of the unspecific symptoms and clinical findings, which causes patients to be diagnosed in advanced disease stages where treatment possibilities are limited (1). In the past few years, progress has been made in the treatment of both AL and ATTR amyloidosis, with development of new and promising therapeutic options (2–7). However, the poor prognosis in patients diagnosed with advanced CA has not yet been overcome, and earlier diagnosis is necessary to make these patients benefit from the therapeutic improvements.

Therefore, accurate diagnostic methods that promote early diagnosis of CA are crucial. Endomyocardial biopsy is considered the gold standard for diagnosis of CA, even though the method is invasive and amyloid deposits can be missed because of patchy distribution (1). In clinical practice, cardiac involvement is considered evident in cases with biopsy-proven amyloidosis in any localization (mainly fat pad biopsy) together with typical findings on echocardiography (8,9). However, the sensitivity of fat pad biopsy for CA diagnosis is only 15% and around 45% to 65% in wild-type and hereditary ATTR, respectively, and 85% in AL (10,11). Furthermore, findings on echocardiography are not specific for amyloidosis and the method is not sensitive enough to detect early stages of CA.

Magnetic resonance imaging (MRI) is often used to detect CA; however, the method is not suitable in patients with renal impairment (which is quite common in AL-amyloidosis) because of the risk of nephrotoxicity from the gadolinium contrast and may be contraindicated in patients with devices such as pacemaker. There is also a risk that "patchy" distribution of amyloidosis can be missed (1).

Scintigraphy with bone-seeking phosphate derivatives has a very high sensitivity in ATTR-CA, both wild-type and hereditary, and together with the absence of a monoclonal protein, a positive bone scintigraphy performs equally to endomyocardial biopsy for the diagnosis of ATTR-CA (12). However, the method is not useful in AL-CA, where most cases are negative and was only evaluated in subjects where echocardiography or cardiac MRI had already shown suspected amyloidosis. Thus, the ability of the method to detect early stages of CA is unclear.

The positron emission tomography (PET) tracer [^{18}F] florbetapir has shown promising diagnostic performance, although there are still no larger studies in cardiac amyloidosis (13,14).

Pittsburgh compound B, [^{11}C]PIB, is the original amyloid-binding tracer for PET and was constructed to detect brain amyloid deposits in vivo in Alzheimer disease (15). The diagnostic utility of PIB-PET in CA has been examined in 5 smaller, single-center studies indicating promising diagnostic performance (16–20). However, the method has not been evaluated in multicenter settings and has not been prospectively applied to clinical cases.

The aim of our dual-center study was to further examine PIB-PET in a larger cohort of amyloidosis patients and controls than what has previously been studied to establish the sensitivity and specificity of the method. We also included a prospective cohort of amyloidosis patients without increased wall thickness on echocardiography to examine the performance of PIB-PET in detection of early CA.

METHODS

SUBJECTS. Thirty-six patients with known CA were included in the study, 15 with AL and 21 with ATTR amyloidosis (16 wild-type and 5 hereditary). There were 2 control groups consisting of healthy volunteers (n = 8) and patients with non-amyloid cardiac hypertrophy (n = 7). CA and control subjects were used to establish cutoff values for the 2 previously proposed, semiquantitative approaches to measuring [^{11}C]PIB uptake in the myocardium.

The best cutoff values were then prospectively applied to 11 patients with evidence of amyloid systemically but without known cardiac involvement (5 patients with AL amyloidosis and 6 with transthyretin mutation). No subject had previously undergone PIB-PET.

In the CA groups, diagnosis was confirmed either by endomyocardial biopsy (n = 24) or by abdominal fat pad biopsy together with echocardiography (n = 12). According to the definition of organ involvement by Gertz et al. (8), cardiac amyloidosis was defined as left ventricular wall thickness >12 mm, with no other cause of hypertrophy such as hypertension. One of the CA patients with AL amyloidosis

TABLE 1 Subject Characteristics, PET, and Echocardiography Data According to Study Group

	AL (n = 15)		ATTR (n = 21)		Hypertrophic Controls (n = 7)		Health Controls (n = 8)		Prospective Group (n = 11)		p Value*	
Male/female	11/4		19/2		5/2		2/6		8/3			
Age (yrs)	69 (10.0)		76 (12.5)		68 (5.0)		53 (11.0)		55 (23.0)			
Positive endomyocardial biopsy	7		17		0		0		2			
Ischemic heart disease	1		6		1		0		0			
Atrial arrhythmia	1		6		3		0		0			
Diuretic use	7		15		1		0		3			
Beta-blocker use	5		12		7		0		0			
ACE-inhibitor/ARB use	6		5		5		0		3			
NYHA functional class I/II/III	3/4/8		2/8/11		2/3/2		-		10/1/0			
NT-proBNP (ng/l)	2,973 (2,485)		3,638 (5,449)		376 (1,089)		ND		77 (605)			
	Reader		Reader		Reader		Reader		Reader		Reader	
PET data	1	2	1	2	1	2	1	2	1	2	1	2
Visually positive	15	15	21	21	0	0	0	0	7	6		
SUV ratio 10–20 min	2.61 (2.61)	1.60 (1.8)	1.64 (0.62)	1.3 (0.73)	0.88 (0.26)	0.63 (0.12)	0.87 (0.26)	0.94 (0.14)	1.16 (0.40)	1.12 (0.36)	**<0.001**	**<0.001**
Retention index 10–20 min (min^{-1})	0.086 (0.075)	0.065 (0.063)	0.045 (0.014)	0.045 (0.01)	0.029 (0.005)	0.024 (0.004)	0.033 (0.005)	0.032 (0.006)	0.040 (0.011)	0.039 (0.007)	**<0.001**	**<0.001**
Echocardiography data												
Interventricular septum (mm)	16 (4)		20 (9)		16 (2)		7.5 (4)		10 (2)		**0.048**	
LV ejection fraction	0.61 (0.12)		0.56 (0.16)		0.67 (0.19)		0.67 (0.10)		0.64 (0.09)		0.158	
LV mass (g/m^2)	127 (50)		123 (99)		121 (43)		66 (20)		79 (39)		0.819	
LV diastolic diameter (mm)	41 (8)		46 (7)		43 (11)		44 (6)		52 (15)		0.125	
LV global longitudinal strain	13 (8)		11 (3)		14 (6)		21 (4)		15 (8)		0.057	
LA volume (ml/m^2)	35 (12)		48 (28)		35 (28)		34 (8)		31 (19)		**0.027**	
TAPSE (mm)	16 (6)		16 (11)		19 (9)		26 (5)		24 (5)		0.418	
E/A ratio	1.8 (2.3)		2.2 (2.6)		0.7 (0.5)		1.2 (0.9)		1.6 (0.7)		**0.015**	
E′ septum	5.0 (3.1)		4.0 (1.7)		4.0 (1.0)		8 (2.5)		9.2 (3.5)		0.173	
E/E′	16 (7)		21 (9)		19 (13)		7.5 (2.8)		8.8 (5.0)		0.187	

Values are median (interquartile range) or n. *Kruskal-Wallis test comparing AL, ATTR, and hypertrophic controls. Statistically significant values ($p < 0.05$) are in **bold**.

ACE = angiotensin-converting enzyme; AL = light chain amyloidosis; ARB = angiotensin receptor blocker; ATTR = transthyretin amyloidosis; E/A = ratio of the Doppler peak velocity of E- and A-wave; E′ = early relaxation velocity on tissue Doppler; E/E′ = early filling velocity divided by the early relaxation velocity; LA = left atrial; LV = left ventricular; ND = not done; PET = positron emission tomography; SUV = standardized uptake value; TAPSE = tricuspid annular plane systolic excursion.

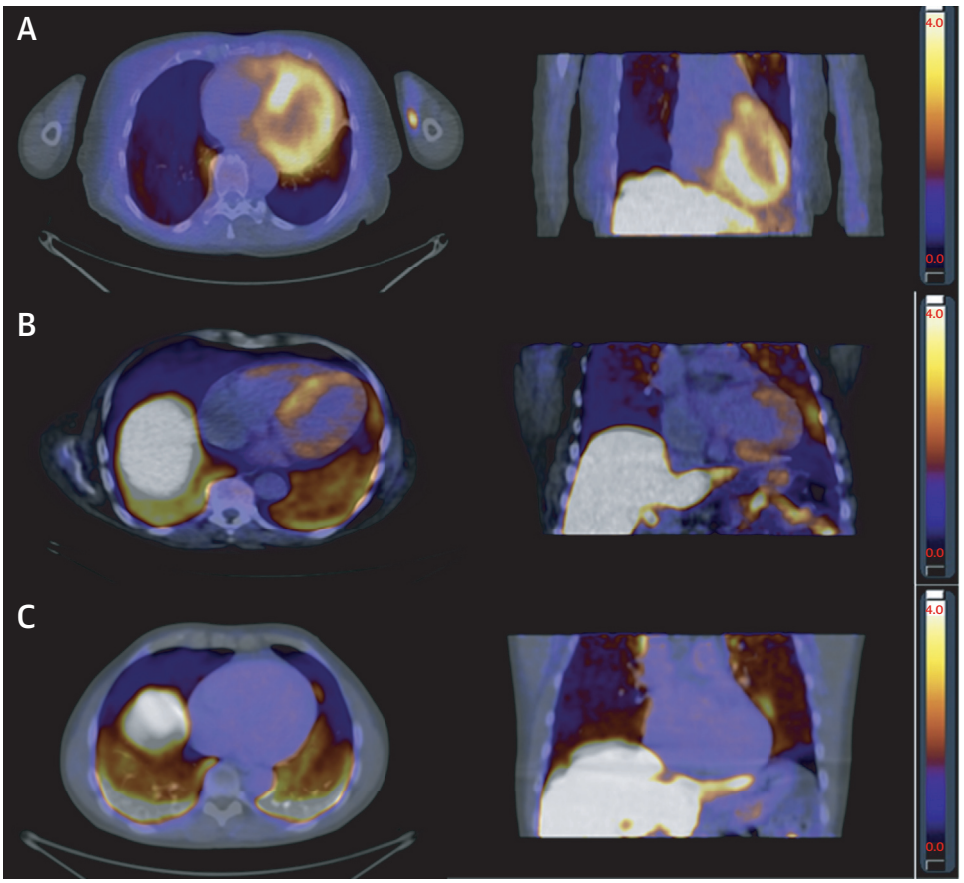
had a positive fat pad biopsy and typical MRI findings for cardiac amyloidosis, although echocardiography showed no increased wall thickness. Twelve of the 15 AL-CA patients had received cytotoxic therapy before enrollment in the study, and 3 were untreated. Among the hereditary ATTR-CA subjects, 3 had the Danish Leu111Met mutation and 2 had the Swedish His88Arg mutation. In the prospective group, all 6 transthyretin mutation carriers had the Leu111Met mutation. The penetrance of this mutation is known to be 100% and cardiac involvement is usually noted between 40 and 55 years of age (21). The median age of the studied subjects with Leu111Met mutation was 48 years (range 45 to 54 years) in the CA group, and 40 years (range 27 to 55 years) in the prospective group. The His88Arg mutation causes late onset cardiomyopathy (≥50 years of age) (22), and the 2 studied patients with this mutation were 67 and 63 years of age.

The hypertrophic control group comprised of patients with cardiac hypertrophy but without any clinical suspicion of amyloidosis. In 3 of the patients, hypertrophy was caused by hypertension and 4 patients had idiopathic hypertrophic cardiomyopathy.

The healthy controls were volunteers with no medical history of cardiac disease or hypertension. Volunteers older than 65 were not included because of the increasing incidence of wild-type ATTR amyloidosis with age (23).

All subjects were examined with PIB-PET and a consecutive echocardiogram was performed within 1 to 2 weeks of PET. Except for the healthy controls, subjects also had blood samples, blood pressure, and ECG taken, and were clinically assessed regarding New York Heart Association (NYHA) functional classification. Informed consent was obtained from all subjects and the study was performed with the approval of the local ethics committees (the Regional

FIGURE 1 Examples of Summed PIB-PET Images Taken 10 to 20 Min After Injection of [^{11}C]PIB



The signal represents myocardium/blood SUV ratio, and the color scale ranges from black (SUV ratio 0) to white (SUV ratio 4.0). Transaxial and coronal view of **(A)** a patient with AL amyloidosis and high degree of [^{11}C]PIB uptake in the left ventricle wall and septum; **(B)** a patient with ATTR amyloidosis and moderate degree of [^{11}C]PIB uptake in the cardiac walls, most apparent in the septum, and **(C)** a healthy volunteer with no myocardial [^{11}C]PIB uptake. All subjects show high signal in the liver, which is due to normal metabolization of [^{11}C]PIB, and in the lungs, which is most likely caused by tracer lipophilicity. ATTR = transthyretin amyloidosis; PET = positron emission tomography; PIB = Pittsburgh compound B; SUV = standardized uptake value.

Ethics Committee in Uppsala and the Central Jutland Regional Committee on Health Research and Ethics). **Table 1** presents an overview and characteristics of the study groups, and additional characteristics of each individual subject is presented in Supplementary Table 1.

PET/CT AND ECHOCARDIOGRAPHY. The study was performed at 2 sites (Uppsala, Sweden, and Aarhus, Denmark) where subjects were examined according to identical protocols. Subjects in Uppsala were scanned with a Discovery ST or MI PET/CT (GE Healthcare, Waukesha, Wisconsin) and subjects in Aarhus with a Biograph Truepoint TrueV 64 PET/CT (Siemens, Erlangen, Germany). After low-dose computed tomography scanning, [^{11}C]PIB (5 MBq/kg) was injected intravenously, and simultaneously a dynamic emission scan of the heart was started and continued for 35 min. Images were reconstructed according to standard settings provided by the vendors, using all relevant corrections, and divided into 31 timeframes of increasing duration (12 × 5, 6 × 10, 4 × 30, 2 × 60, 2 × 120, and 5 × 300 s).

Image analysis was performed with Carimas software version 2.63 (Turku, Finland) as previously described (24). Regions of interest were manually placed in the left atrial blood pool and left ventricular wall, from which time-activity curves were derived. Images were defined as positive or negative for amyloid presence by qualitative visual inspection. Summed images from 10 to 20 min after [^{11}C]PIB

injection were also evaluated semiquantitatively by calculating a myocardium/blood standardized uptake value ratio (SUVR). For calculation of the [^{11}C]PIB retention index (RI), the mean tissue concentration between 10 and 20 min was divided by the integral of the blood time-activity curve from 0 to 15 min after injection. All PIB-PET examinations were evaluated by 2 independent observers, 1 at each study site, who were blinded regarding the diagnosis of the subjects. The degree of agreement between the 2 different readers was good, with an intraclass correlation coefficient of 0.73 (95% confidence interval [CI]: 0.54 to 0.84) for SUVR and 0.93 (95% CI: 0.88 to 0.96) for RI.

Echocardiography was performed by experienced investigators according to current guidelines (25). Measurements included for example interventricular septal wall thickness (IVST), tricuspid annular plane systolic excursion (TAPSE), left ventricular ejection fraction (LVEF) and left ventricular global longitudinal strain, all of which have been previously associated with outcome in CA (26).

STATISTICAL ANALYSIS. IBM SPSS 23 and SAS JMP 14 were used for statistical analysis. Median was used as the measure of central tendency, and interquartile range (IQR), the difference between 75th and 25th percentiles, for statistical dispersion. The Mann-Whitney *U* test and Kruskal-Wallis test were used for group comparison. Spearman rank-order test and ordinal logistic regression were used to evaluate correlations of [^{11}C]PIB uptake with clinical and echocardiographic parameters. Receiver operating characteristic (ROC) curves were analyzed to determine optimal cutoff values that could differentiate the study groups with the highest sensitivity and specificity. Positive and negative predictive values as well as accuracy were calculated. The p values < 0.05 were considered statistically significant.

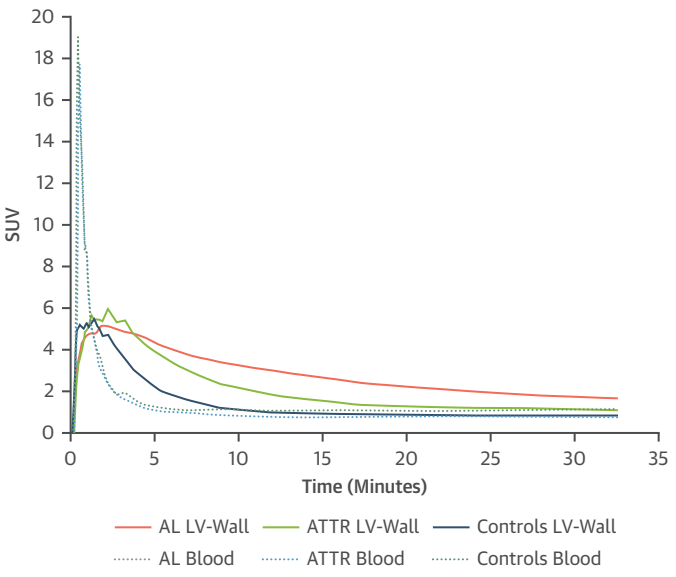
RESULTS

VISUAL ASSESSMENT. At visual inspection of the summed PET images at around 10 to 20 min after [^{11}C]PIB injection, all known CA patients, both AL and ATTR, were [^{11}C]PIB positive. In contrast, none of the hypertrophic or healthy controls showed visible [^{11}C]PIB uptake. Figure 1 shows examples of PET images used for visual assessment.

STANDARDIZED UPTAKE VALUE. The myocardium to blood SUV ratio was calculated for all time frames, and was higher in CA patients than in controls from 3.5 min after [^{11}C]PIB injection (Figure 2). This is demonstrated by a larger separation between the myocardium and blood curves. The ratio was higher in AL than in ATTR patients ($p < 0.001$), but with a larger variability among AL patients. The largest difference between amyloidosis patients and controls was seen at 10 to 20 min after [^{11}C]PIB injection. At this time point, the median SUVR was 2.61 (IQR: 2.61) in AL patients; 1.64 (IQR: 0.62) in ATTR; 0.88 (IQR: 0.26) in the hypertrophic controls; and 0.87 (IQR: 0.26) in the healthy controls, with a significantly higher ratio ($p < 0.001$) in CA than in controls (Central Illustration).

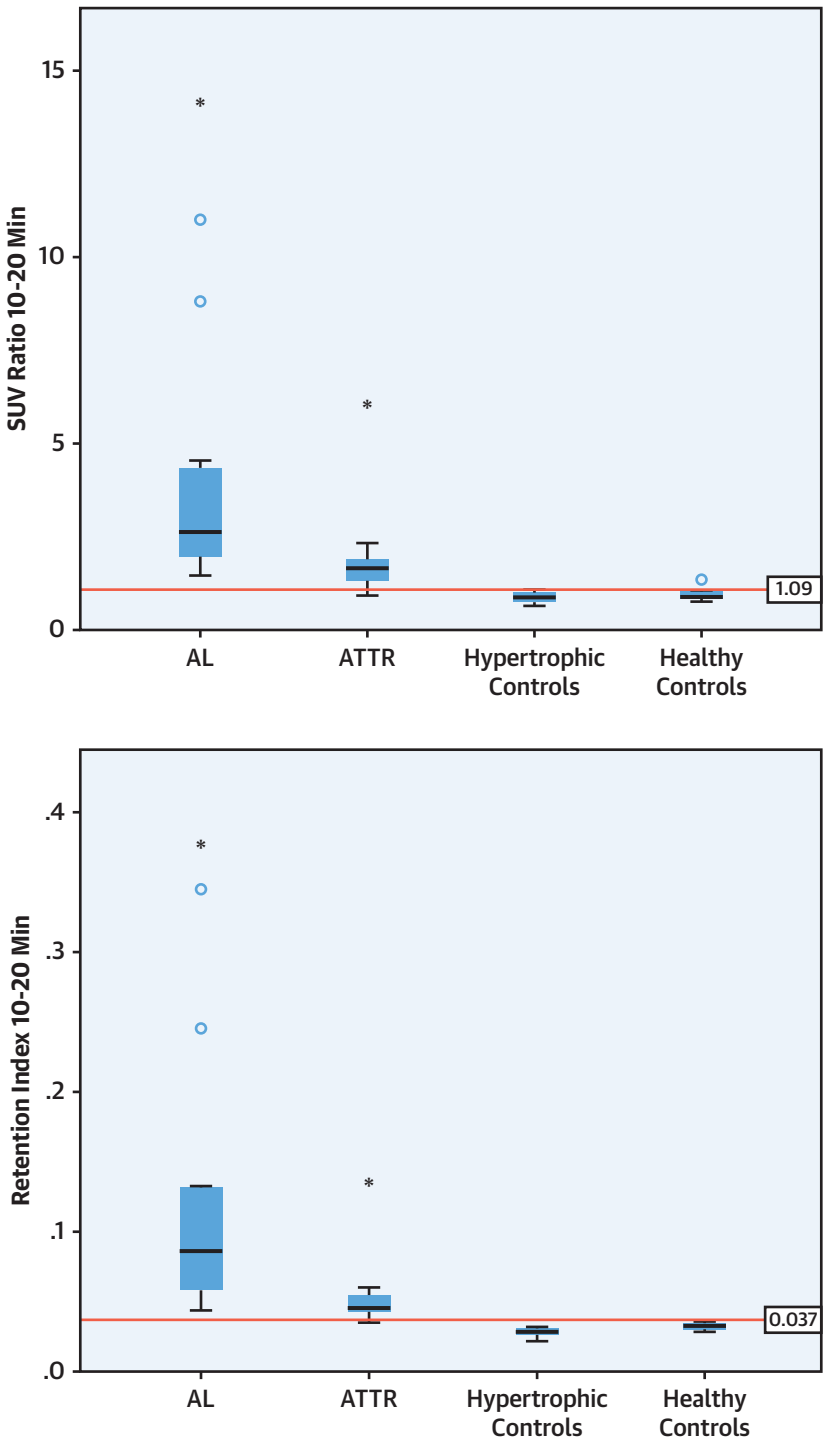
With an SUVR cutoff at 1.09, the area under the curve (AUC) of the ROC curve was 0.98 (95% CI: 0.94 to 1.00), discriminating CA patients (AL and ATTR) from controls (hypertrophic and healthy) with 94% (95% CI: 80% to 99%) sensitivity and 93% (95% CI: 66 to 100) specificity (Table 2). The positive predictive value with this cutoff was 97% (95% CI: 83% to 100%) and the negative predictive value 88% (95% CI: 60% to 98%). The method's accuracy was 94% (95% CI: 84% to 99%). A cutoff SUVR of 1.4 completely differentiated AL amyloidosis from controls with 100% (95% CI: 88% to 100%) accuracy. When discriminating ATTR patients from controls, a cutoff value of 1.09 yielded 91% (95% CI: 68% to 98%) sensitivity and 93% (95% CI: 66% to 100%) specificity, AUC of the ROC curve was 0.96 (95% CI: 0.90 to 1.00). The positive predictive value with this cutoff was 95% (95% CI: 73% to 100%) and the negative predictive value 88% (95% CI: 60% to 98%). Accuracy was 92% (95% CI: 78% to 98%).

FIGURE 2 SUV Time Curves for Arterial Blood and LV Wall



SUV represents median values of the patients with AL and ATTR amyloidosis, and the controls (hypertrophic and healthy together). Time is minutes after injection of [^{11}C]PIB. AL = light chain amyloidosis; LV = left ventricle; other abbreviations as in Figure 1.

CENTRAL ILLUSTRATION **SUV Ratio (Myocardium to Blood) and Retention Index (min^{-1}) for the Different Study Groups, 10 to 20 min After [^{11}C]PIB Injection**



Rosengren, S. et al. J Am Coll Cardiol Img. 2020;■(■):■-■.

Analysis includes the patients with known CA, but not AL patients or TTR mutants without increased wall thickness. The **red reference line** represents the cutoff SUV ratio 1.09 and retention index 0.037 min^{-1}. **Circles** represent outliers, and **stars** show extreme outliers. AL = light chain amyloidosis; ATTR = transthyretin amyloidosis; CA = cardiac amyloidosis; PIB = Pittsburgh compound B; SUV = standardized uptake value.

TABLE 2 Sensitivity and Specificity Data From ROC Curves, Differentiating the Stated Study Groups

	Cutoff (min^{-1})	Sensitivity (%)	95% CI (%)	Specificity (%)	95% CI (%)	AUC	95% CI
SUV Ratio 10-20 min							
Reader 1							
CA: controls	1.09	94	80-99	93	66-100	0.98	0.94-1.00
AL-CA: controls	1.40	100	75-100	100	75-100	1.00	1.00-1.00
ATTR-CA: controls	1.09	91	68-98	93	66-100	0.96	0.90-1.00
Reader 2							
CA: controls	0.95	94	80-99	93	66-100	0.97	0.94-1.00
AL-CA: controls	1.12	100	75-1.00	100	75-100	1.00	1.00-1.00
ATTR-CA: controls	0.95	91	68-98	93	66-100	0.96	0.86-1.00
Retention index 10-20 min							
Reader 1							
CA: controls	0.037	94	80-99	100	75-100	1.00	0.99-1.00
AL-CA: controls	0.040	100	75-100	100	75-100	1.00	1.00-1.00
ATTR-CA: controls	0.035	100	81-100	93	66-100	1.00	0.98-1.00
Reader 2							
CA: controls	0.039	94	80-99	93	66-100	0.97	0.91-1.00
AL-CA: controls	0.039	100	75-100	93	66-100	0.99	0.97-1.00
ATTR-CA: controls	0.039	91	68-98	93	66-100	0.95	0.87-1.00

Analysis includes the patients with known CA, but not AL patients and TTR mutation carriers without increased wall thickness. "Controls" represents both hypertrophic and healthy controls together.
AUC = area under the curve; CA = cardiac amyloidosis; CI = confidence interval; ROC = receiver-operating characteristic; other abbreviations as in Table 1.

RETENTION INDEX. The myocardial RI between 10 and 20 min was significantly higher in CA patients than in controls ($p < 0.001$) (Central Illustration). The median RI was 0.086 (IQR: 0.075) min^{-1} in AL patients; 0.045 (IQR: 0.014) min^{-1} in ATTR; 0.029 (IQR: 0.005) min^{-1} in the hypertrophic controls, and 0.033 (IQR: 0.005) min^{-1} in the healthy controls. RI could also completely discriminate AL-CA from controls (both hypertrophic and healthy), with the cutoff value of 0.040 min^{-1} (Table 2). Combining all CA and control subjects, the cutoff value 0.037 min^{-1} yielded 94% (95% CI: 80% to 99%) sensitivity and 100% (95% CI: 75% to 100%) specificity. The positive predictive value was 100% (95% CI: 87% to 100%) and negative predictive value 88% (95% CI: 62% to 98%). Accuracy was 96% (95% CI: 87% to 100%).

TABLE 3 Characteristics and Results of Each Subject in the Prospective Study Group

Gender	Race	Age (yrs)	Diagnosis	Positive EMB	NYHA Functional Class	NT-proBNP (ng/l)	Troponin T (ng/l)	Visually PET Positive†	SUV Ratio	Retention Index (min^{-1})	Echo IVST (mm)
Male	Caucasian	58	AL	Yes*	2	734	19	‡	0.88	0.032	11
Male	Caucasian	70	AL	No	1	-	-	Yes	1.19	0.04	9
Male	Caucasian	69	AL	No	1	649	20	Yes	1.69	0.074	10
Male	Caucasian	60	AL	No	1	443	62	Yes	1.18	0.044	11
Male	Caucasian	60	AL	No	1	75	18	No	1.36	0.03	10
Male	Caucasian	53	ATTR Leu111Met	No	1	60	14	‡	1.05	0.039	9
Female	Caucasian	55	ATTR Leu111Met	Yes	1	1,070	25	Yes	1.25	0.044	11
Female	Caucasian	27	ATTR Leu111Met	No	1	73	6	No	0.85	0.045	8
Male	Caucasian	30	ATTR Leu111Met	No	1	37	6	No	0.70	0.034	10
Female	Caucasian	37	ATTR Leu111Met	No	1	78	6	Yes	0.78	0.04	8
Male	Caucasian	42	ATTR Leu111Met	No	1	67	6	‡	1.16	0.034	9

*EMB showed amyloid confined to the vessels. †Yes or no indicate positive or negative by both readers. ‡Disagreement between reader 1 and 2.
EMB = endomyocardial biopsy; IVST = interventricular septum thickness; NYHA = New York Heart Association; other abbreviations as in Table 1.

TABLE 4 Associations Of Semiquantitative Estimates Of Myocardial [^{11}C]PIB Uptake With Clinical and Echocardiographic Parameters

	AL				ATTR				Combined Amyloidosis			
	SUV Ratio		RI		SUV Ratio		RI		SUV Ratio		RI	
Ordinal Logistic Regression	**Chi-Square**	**p Value**	**Chi-Square**	**p Value**	**Chi-Square**	**p Value**	**Chi-Square**	**p Value**	**Chi-Square**	**p Value**	**Chi-Square**	**p Value**
NYHA functional class (I/II/III)	0.15	0.69	0.36	0.55	**8.3**	**0.004**	**8.2**	**0.004**	0.67	0.41	0.66	0.42
Spearman rank correlation	rho	p	rho	p	rho	p	rho	p	rho	p	rho	p
NT-proBNP	0.33	0.17	0.23	0.35	**0.56**	**0.003**	**0.54**	**0.005**	0.39	0.008	0.36	0.02
Interventricular septal thickness	**0.62**	**0.004**	**0.55**	**0.01**	**0.51**	**0.006**	0.28	0.15	0.38	0.009	0.23	0.12
LV ejection fraction	0.14	0.56	0.17	0.46	**-0.56**	**0.002**	-0.32	0.11	-0.19	0.21	-0.04	0.78
LV mass/m^2	0.32	0.18	0.24	0.31	**0.55**	**0.003**	0.39	0.05	0.40	0.005	0.28	0.06
LV diastolic diameter	**-0.52**	**0.02**	**-0.56**	**0.01**	-0.20	0.32	-0.28	0.16	-0.39	0.008	-0.47	0.001
LV global longitudinal strain	0.18	0.44	0.27	0.26	-0.24	0.23	-0.25	0.21	-0.01	0.93	0.03	0.87
LA volume/m^2	-0.27	0.26	-0.44	0.06	0.44	0.02	0.38	0.05	0.04	0.81	-0.09	0.56
TAPSE	**-0.61**	**0.004**	**-0.55**	**0.01**	**-0.63**	**<0.001**	**-0.51**	**0.007**	**-0.60**	**<0.001**	**-0.55**	**<0.001**
E/A ratio	0.05	0.85	-0.03	0.89	0.20	0.35	0.37	0.08	0.11	0.46	0.14	0.36
E′ septum	-0.39	0.09	-0.31	0.18	**-0.67**	**<0.001**	-0.45	0.02	-0.42	0.003	-0.28	0.06
E/E′	0.31	0.18	0.21	0.37	**0.57**	**0.002**	0.42	0.03	0.34	0.02	0.24	0.11

Correlation coefficients (rho) <-0.5 or >0.5 with p values <0.05 are presented in **bold**.
RI = retention index; other abbreviations as in Tables 1 and 3.

There was no significant difference between the hypertrophic and healthy controls, either in SUVR ($p = 0.694$) or in RI ($p = 0.054$).

PROSPECTIVE GROUP. Among the amyloidosis patients without increased wall thickness, 5 of 11 subjects were unanimously judged as visually [^{11}C]PIB positive by the 2 readers, 2 of 6 transthyretin mutation carriers and 3 of 5 AL patients (Table 3). Three of the 11 prospective subjects were classified as [^{11}C]PIB positive by 1 of the readers but not the other. Median RI was higher in the predisposed patients without increased wall thickness compared with controls ($p = 0.001$) (Table 1). In 2 of the prospective patients, endomyocardial biopsies were performed at follow-up after PIB-PET. One PET-positive transthyretin mutation carrier with normal echocardiography and no symptoms had an amyloid-positive endomyocardial biopsy at follow-up. In 1 PET-negative AL patient without increased wall thickness, but with low LVEF and NYHA functional class II, endomyocardial biopsy was positive for amyloid confined to the vasculature, this patient has been described in a case report by Clemmensen et al (27).

ASSOCIATIONS WITH ECHOCARDIOGRAPHY AND CLINICAL PARAMETERS. In the ATTR group, both SUVR and RI were significantly associated with NYHA functional class (both $p = 0.004$); NT-proBNP levels ($p \leq 0.005$) and TAPSE ($p \leq 0.007$) (Table 4). In addition, SUVR was associated with IVST ($p = 0.006$), LVEF ($p = 0.002$), left ventricular mass ($p = 0.003$), E′, and E/E′ ($p \leq 0.002$). In the AL cohort, both SUVR and RI were significantly associated with IVST ($p \leq 0.01$) left ventricular diastolic diameter ($p \leq 0.02$) and TAPSE ($p \leq 0.01$). In the combined amyloidosis group, there was an association between TAPSE and both SUVR and RI ($p < 0.001$), but no correlation to any other clinical or echocardiographic parameter.

DISCUSSION

To date, this dual-site study composes the largest number of CA patients examined with PIB-PET. It is also the first [^{11}C]PIB study with a control group with non-amyloid-induced hypertrophic myocardium. The main finding of this study was the high sensitivity (94%) and specificity (93% to 100%) of PIB-PET for distinguishing cardiac amyloidosis patients from both hypertrophic patients and healthy controls. When viewed by experienced professionals, visual interpretation alone achieved an accuracy of 100% in this cohort. The high accuracy in this study is encouraging, considering that different sites, scanners, and observers were used. This suggests that the use of PIB-PET could be the predominant method for assessing cardiac involvement in drug trials, similar to the same tracer's use in determining Alzheimer disease (28), it also suggests that PIB-PET can be of clinical value for CA diagnosis. Including this study, there are published reports on a total number of 137 unique cardiac PIB-PET examinations. These reports have shown that the method is 89% to 100% accurate in detecting cardiac amyloidosis (16-20). In comparison, a recent meta-analysis on the accuracy of late gadolinium enhancement on cardiac MRI showed a

summary sensitivity of 85% and specificity of 92% (29). This makes PIB-PET probably at least comparable to contrast-enhanced MRI, as a diagnostic tool in CA. Because [^{11}C]PIB binds directly to amyloid, PIB-PET can detect amyloidosis on a molecular level, as opposed to MRI and echocardiography, which mainly show indirect signs of amyloidosis. PIB-PET is thereby able to detect amyloid even when distribution is "patchy," cases in which MRI (and endomyocardial biopsies) may be misleading.

Another finding in this study was the high prevalence of PIB uptake among the amyloidosis patients without increased cardiac wall thickness (both AL and ATTR), indicating that PIB-PET may be able to detect early stages of CA. Similar findings were reported from a study including 10 patients with transthyretin mutations and inconclusive echocardiographic findings, where all patients were [^{11}C]PIB positive (20). Thus, PIB-PET may be useful for early diagnosis and treatment initiation, which is of great importance to counter the dismal prognosis associated with CA. The availability of highly accurate imaging tools for earlier diagnosis appears particularly relevant in the light of the recent recognition of amyloidosis as an underestimated cause of heart failure with preserved ejection fraction (30), and treatment advances both in AL (2–4) and ATTR amyloidosis (5–7).

A recent multicenter study using bone scintigraphy reported a >99% sensitivity and 86% specificity for the diagnosis of ATTR-CA, and specificity increased to 100% when a positive bone scintigraphy was combined with the absence of a monoclonal protein (12).

Unlike bone scintigraphy, PIB-PET detects CA in both AL and ATTR patients, with higher [^{11}C]PIB retention in the AL patients in our study. The method was able to completely distinguish AL amyloidosis from both non-CA hypertrophic patients and healthy volunteers, with 100% accuracy by simple semiquantitative indices or visual inspection. Thus, in clinical practice, PIB-PET might have its greatest value in diagnosis of AL-CA where bone scintigraphy is not a reliable method. Furthermore, the proposed nonbiopsy diagnosis of ATTR-CA with bone scintigraphy required the suspicion of CA on echocardiography or MRI, both of which show signs of CA quite late in the disease process. A possible clinical use of PIB-PET could thereby be for early detection of cardiac CA, whereas the role of scintigraphy may be to distinguish between amyloid types.

Visual inspection of a PET image obtained around 10 to 20 min after [^{11}C]PIB injection works well for distinguishing CA patients from controls. The reason for the better accuracy of visual inspection is because CA often presents with heterogeneous distribution of [^{11}C]PIB, and uptake in smaller areas might be missed by using a more global LV/blood ratio. In cases where uptake is difficult to assess visually, comparison of the time-activity curves of myocardium and blood (where higher myocardial activity compared with blood at the time interval 10 to 20 min indicates [^{11}C]PIB uptake), as well as semiquantitative measures such as SUVR and RI, can be useful. The results of this study suggest that, at the time interval of 10 to 20 min, cutoff values of 1.09 for the SUVR and 0.037 min^{-1} for RI can be used. A recent study of [^{11}C]PIB kinetics showed that the simplified measures SUV and RI were highly correlated to results from fully quantitative measurements with arterial blood sampling and metabolite analysis. This suggests that these semiquantitative methods work well, and metabolite correction is not regarded as necessary (31). In clinical practice, we suggest that visual inspection at around 10 to 20 min is used at first hand. As a semiquantitative method, we recommend the simple measure SUVR, using the cutoff 1.09 for PIB-PET positivity.

There is no specific binding of [^{11}C]PIB to myocardium without amyloidosis (16), but [^{11}C]PIB signal was not 0 in the control groups (**Central Illustration**), which can be explained by spill-in of radioactivity from the blood pool and surrounding organs into the cardiac regions of interest.

The production of [^{11}C]PIB requires a cyclotron nearby, which limits utility to larger hospitals. However, [^{11}C]PIB is already available in many facilities worldwide because it is a standard tool for Alzheimer diagnosis. Compared with cardiac biopsy, PET is a noninvasive method without significant patient risks, and with possibly shorter response times compared with the more time-consuming histopathological examination. The cost is generally higher than other imaging modalities, and the added value of early diagnosis with [^{11}C]PIB PET for directing amyloid-targeting therapies should be evaluated in future studies.

A method for grading the CA burden would be of clinical value because there is currently no effective imaging method for follow-up after amyloidosis treatment. Lee et al. (17) found a significantly higher [^{11}C]PIB uptake in chemotherapy-naïve AL patients compared with chemotherapy-treated patients, suggesting that the method could be used to assess disease burden. This could not be reproduced in our study, because most AL patients had been previously treated. In the current study, we found some associations between [^{11}C]PIB uptake and measures of

cardiac function, suggesting that [^{11}C]PIB measurements may be indicative of amyloid burden to some extent. However, the degree of [^{11}C]PIB retention is strongly influenced by the type of amyloid fibrils. This was seen in our study, where [^{11}C]PIB uptake was highest in AL patients. Pilebro et al. (20) reported a difference in [^{11}C]PIB retention in hereditary ATTR amyloidosis depending on the type of amyloid fibrils, with higher uptake in patients with full-length fibrils than in patients with fragmented fibrils. Thus, there seems to be a difference in the binding of [^{11}C]PIB depending on the type of amyloid fibrils; further studies are needed to elucidate the relevance of this finding.

Myocardial blood flow could also theoretically influence the degree of [^{11}C]PIB retention, with possibly lower delivery of [^{11}C]PIB to the tissue in patients with poor myocardial perfusion or scarring. This could possibly contribute to the lower [^{11}C]PIB uptake in ATTR compared to AL because the thicker cardiac walls seen in ATTR could be associated with lower perfusion. However, in a previous small study (16), there was no significant correlation between [^{11}C]PIB retention and myocardial blood flow as assessed by PET. Further studies with follow-up PET examinations after amyloidosis treatment would be needed to evaluate PIB-PET as a tool for evaluating treatment efficacy.

STUDY LIMITATIONS. In our study, only two-thirds of the CA patients had endomyocardial biopsies performed. For the remaining patients, echocardiography was used together with a noncardiac biopsy as reference. Had endomyocardial biopsy been performed on all subjects, there could possibly have been more false-negative patients with PIB-PET.

Furthermore, even though this is the largest PIB-PET study in CA, the patient groups are still small and the confidence intervals around the point estimates for sensitivity and specificity are wide. The prospective group includes only 11 subjects and, although our results complement the findings of Pilebro et al., more studies on [^{11}C]PIB-PET in early CA detection are needed to define the diagnostic accuracy in this setting.

The CA groups in this study are heterogeneous, consisting of patients in different stages of disease, some newly diagnosed and some in late disease stages. Among the AL-CA patients, there are both treatment-naïve and chemotherapy-treated patients, the majority having received amyloidosis treatment. It is likely that if all AL patients were untreated, there would be even higher PIB uptake in this group. There is also an imbalance in terms of gender, with only 6 female CA subjects, which makes it statistically uncertain to control for possible gender differences when it comes to cardiac structure and function parameters.

CONCLUSIONS

[^{11}C]PIB-PET was an excellent method to distinguish both ATTR and AL subtypes of cardiac amyloidosis from healthy and hypertrophied controls, with high accuracy for both simple visual analysis and semi-quantitative measurements. The method performed exceptionally well in AL cardiac amyloidosis, where accuracy was 100%. [^{11}C]PIB uptake was also seen in a subgroup of amyloidosis patients without increased wall thickness, indicating that PIB-PET may be able to detect early stages of cardiac involvement. [^{11}C]PIB uptake was somewhat associated with symptoms and signs of cardiac dysfunction, and may potentially reflect disease burden, although further studies are needed to evaluate the role of PIB-PET in follow-up of CA patients.

ADDRESS FOR CORRESPONDENCE: Dr Sara Rosengren, Department of Hematology, Ing 100, pl 2 Akademiska sjukhuset, 751 85 Uppsala, Sweden. E-mail: sara.rosengren@akademiska.se.

PERSPECTIVES

COMPETENCY IN MEDICAL KNOWLEDGE: [^{11}C]PIB PET is a sensitive method for visualization of cardiac amyloidosis, with 100% accuracy in AL amyloidosis. The method may be able to detect early stages of cardiac amyloidosis.

COMPETENCY IN PATIENT CARE AND PROCEDURAL SKILLS: When investigating patients with suspected cardiac amyloidosis, PIB-PET is a sensitive and accurate, noninvasive method that is especially relevant in detection of early disease stages, and when AL amyloidosis is suspected.

TRANSLATIONAL OUTLOOK: Even though there seems to be associations between [^{11}C]PIB uptake and cardiac function, further studies are needed to examine whether [^{11}C]PIB-PET can be used as a method for follow-up after amyloidosis treatment.

REFERENCES

1. Grogan M, Dispenzieri A, Gertz MA. Light-chain cardiac amyloidosis: strategies to promote early diagnosis and cardiac response. Heart 2017;103:1065–72.

2. Sanchorawala V, Palladini G, Kukreti V, et al. A phase 1/2 study of the oral proteasome inhibitor ixazomib in relapsed or refractory AL amyloidosis. Blood 2017;130:597–606.

3. Kaufman GP, Schrier SL, Lafayette RA, Arai S, Witteles RM, Liedtke M. Daratumumab yields rapid and deep hematologic responses in patients with heavily pretreated AL amyloidosis. Blood 2017;130:900–2.

4. Palladini G, Milani P, Foli A, et al. Clinical Trials and Observations. A phase 2 trial of pomalidomide and dexamethasone rescue treatment in patients with AL amyloidosis. Blood 2018;129:2120–4.

5. Maurer MS, Schwartz JH, Gundapaneni B, et al. Tafamidis treatment for patients with transthyretin amyloid cardiomyopathy. N Engl J Med 2018;379:1007–16.

6. Benson MD, Waddington-Cruz M, Berk JL, et al. Inotersen treatment for patients with hereditary transthyretin amyloidosis. N Engl J Med 2018;379:22–31.

7. Adams D, Gonzalez-Duarte A, O'Riordan WD, et al. Patisiran, an RNAi therapeutic, for hereditary transthyretin amyloidosis. N Engl J Med 2018;379:11–21.

8. Gertz MA, Comenzo R, Falk RH, et al. Definition of organ involvement and treatment response in immunoglobulin light chain amyloidosis (AL):a consensus opinion from the 10th International Symposium on Amyloid and Amyloidosis. Am J Hematol 2005;79:319–28.

9. Ando Y, Coelho T, Berk JL, et al. Guideline of transthyretin-related hereditary amyloidosis for clinicians. Orphanet J Rare Dis 2013;8:1–18.

10. Fine NM, Arruda-Olson AM, Dispenzieri A, et al. Yield of noncardiac biopsy for the diagnosis of transthyretin cardiac amyloidosis. Am J Cardiol 2014;113:1723–7.

11. Quarta CC, Gonzalez-Lopez E, Gilbertson JA, et al. Diagnostic sensitivity of abdominal fat aspiration in cardiac amyloidosis. Eur Heart J 2017;38:1905–8.

12. Gillmore JD, Maurer MS, Falk RH, et al. Nonbiopsy diagnosis of cardiac transthyretin amyloidosis. Circulation 2016;133:2404–12.

13. Park MA, Padera RF, Belanger A, et al. ^{18}F-florbetapir binds specifically to myocardial light chain and transthyretin amyloid deposits: autoradiography study. Circ Cardiovasc Imaging 2015;8:1–8.

14. Dorbala S, Vangala D, Semer J, et al. Imaging cardiac amyloidosis: a pilot study using 18F-florbetapir positron emission tomography. Eur J Nucl Med Mol Imaging 2014;41:1652–62.

15. Klunk WE, Engler H, Nordberg A, et al. Imaging brain amyloid in Alzheimer's disease with Pittsburgh Compound-B. Ann Neurol 2004;55:306–19.

16. Antoni G, Lubberink M, Estrada S, et al. In vivo visualization of amyloid deposits in the heart with 11C-PIB and PET. J Nucl Med 2013;54:213–20.

17. Lee SP, Lee ES, Choi H, et al. 11C-Pittsburgh B PET imaging in cardiac amyloidosis. J Am Coll Cardiol Img 2015;8:50–9.

18. Minamimoto R, Awaya T, Iwama K, et al. Significance of 11C-PIB PET/CT in cardiac amyloidosis compared with 99mTc-aprotinin scintigraphy: a pilot study. J Nucl Cardiol 2018;45:452–61.

19. Ezawa N, Katoh N, Oguchi K, Yoshinaga T, Yazaki M, Sekijima Y. Visualization of multiple organ amyloid involvement in systemic amyloidosis using 11C-PiB PET imaging. Eur J Nucl Med Mol Imaging 2018;45:452–61.

20. Pilebro B, Arvidsson S, Lindqvist P, et al. Positron emission tomography (PET) utilizing Pittsburgh compound B (PIB) for detection of amyloid heart deposits in hereditary transthyretin amyloidosis (ATTR). J Nucl Cardiol 2018;25:240–8.

21. Hastrup Svendsen I, Steensgaard-Hansen F, Nordvåg BY. A clinical, echocardiographic and genetic characterization of a Danish kindred with familial amyloid transthyretin methionine 111 linked cardiomyopathy. Eur Heart J 1998;19:782–9.

22. Hellman U, Lundgren HE, Westermark P, et al. A genealogical and clinical study of the phenotypical variation within the Swedish transthyretin His88Arg (p. His108Arg) amyloidosis family. Eur J Med Genet 2015;58:211–5.

23. Tanskanen M, Peuralinna T, Polvikoski T, et al. Senile systemic amyloidosis affects 25% of the very aged and associates with genetic variation in alpha2-macroglobulin and tau: a population-based autopsy study. Ann Med 2008;40:232–9.

24. Kero T, Lindsjö L, Sörensen J, Lubberink M. Accurate analysis and visualization of cardiac 11C-PIB uptake in amyloidosis with semiautomatic software. J Nucl Cardiol 2016;23:741–50.

25. Lang RM, Badano LP, Mor-Avi V, et al. Recommendations for cardiac chamber quantification by echocardiography in adults: an update from the American Society of Echocardiography and the European Association of Cardiovascular Imaging. Eur Heart J Cardiovasc Imaging 2015;16:233–71.

26. Knight DS, Zumbo G, Barcella W, et al. Cardiac structural and functional consequences of amyloid deposition by cardiac magnetic resonance and echocardiography and their prognostic roles. J Am Coll Cardiol Img 2019;12:823–33.

27. Clemmensen TS, Mølgaard H, Andersen NF, Baerentzen S, Soerensen J, Poulsen SH. A rare presentation of cardiac amyloid deposits isolated to intramural vessels. Echocardiography 2016;33:1777–80.

28. Rinne JO, Brooks DJ, Rossor MN, et al. 11C-PiB PET assessment of change in fibrillar amyloid-β load in patients with Alzheimer's disease treated with bapineuzumab: a phase 2, double-blind, placebo-controlled, ascending-dose study. Lancet Neurol 2010;9:363–72.

29. Zhao L, Tian Z, Fang Q. Diagnostic accuracy of cardiovascular magnetic resonance for patients with suspected cardiac amyloidosis: a systematic review and meta-analysis. BMC Cardiovasc Disord 2016;16:1–10.

30. González-López E, Gallego-Delgado M, Guzzo-Merello G, et al. Wild-type transthyretin amyloidosis as a cause of heart failure with preserved ejection fraction. Eur Heart J 2015;36:2585–94.

31. Kero T, Sörensen J, Antoni G, et al. Quantification of11C-PIB kinetics in cardiac amyloidosis. J Nucl Cardiol 2018 Jul 23 [E-pub ahead of print].

KEY WORDS diagnosis, heart, nuclear imaging, PET, Pittsburgh compound B

APPENDIX For a supplemental table, please see the online version of this paper.